IEEE Access
Multidisciplinary | Rapid Review | Open Access Journal

Received 10 July 2022, accepted 8 August 2022, date of publication 25 August 2022, date of current version 8 September 2022.

Digital Object Identifier 10.1109/ACCESS.2022.3201488

RESEARCH ARTICLE

Discrimination of Customers Decision-Making in a Like/Dislike Shopping Activity Based on Genders: A Neuromarketing Study

ATEFE HASSANI[1], AMIN HEKMATMANESH[2], AND ALI MOTIE NASRABADI[1]
[1]Department of Biomedical Engineering, Shahed University, Tehran 33191-18651, Iran
[2]Laboratory of Intelligent Machines, LUT University, 53850 Lappeenranta, Finland

Corresponding author: Amin Hekmatmanesh (amin.hekmatmanesh@lut.fi)

This work involved human subjects or animals in its research. Approval of all ethical and experimental procedures and protocols was granted by the Medical Research Ethics Committee (MREC) of Shahed University.

ABSTRACT The present study considers the decision making of customers in a Like/Dislike task with respect to the gender of customers. The investigation is performed by recording electroencephalography (EEG) signal from 20 subjects that stimulated by displaying images of shoes. In the algorithm, the EEG signals were denoised by using artifact subspace reconstruction and independent component analysis methods. The Wavelet technique is then applied to attain five EEG frequency bands and, subsequently linear and nonlinear features were extracted. The extracted features includes linear features, namely the power spectral density and energy of wavelet; and nonlinear features, namely the fractal dimension, entropy, and trajectory volume behavior quantifiers. The meaningfulness of the features for identifying discriminative channels as well as frequency bands is considered by means of Wilcoxon Rank Sum statistical test. The identifications of Like/Dislike conditions were then facilitated by the Support Vector Machine, Random Forest, Linear Discriminant Analysis, and K-Nearest Neighbors classifiers. Results illustrated that higher frequency bands, the combination of theta, alpha, and beta, in Fp1, Fp2, F7, F8, Cz, and Pz regions was observed for female group. The most distinctive feature and classifier for the female group was the energy of the wavelet coefficient and RF classifier, respectively, that produced the highest accuracy rate of $71.51 \pm 5.1\%$. In addition, the most distinctive features for males were sample and approximate entropy, as well as the Higuchi fractal dimension that with the RF classifier produced an accuracy rate of $71.33 \pm 14.07\%$. The nonlinear features investigation revealed more involved brain regions in a Like/Dislike task than the previous studies. In addition, it is revealed that the Like decision-making happens earlier than Dislike.

INDEX TERMS Brain signal, like/dislike, neuromarketing, random forest, support vector machine, linear discriminant analysis, k-nearest neighbors, Wilcoxon Rank Sum.

I. INTRODUCTION

Traditionally, marketing methods (newspaper advertisements and television commercials) were invested based on the customer's spoken information for identifying their interests. In some points, the investors got success but in many cases investments failed.

Neuromarketing is a topic for marketing research area that uses neuroscience-related techniques to study consumers behavior. The concept of neuromarketing was first introduced by psychologist [1] in the 1990s at Harvard University. It is revealed that the decision-making process about unknown brands happens on an unconscious level of mind [2]. Neuromarketing techniques such as electroencephalography (EEG) signal processing has been employed and results are attributed to the human unconscious information during

The associate editor coordinating the review of this manuscript and approving it for publication was Xinyu Du.

shopping activities. The consequence of the neuromarketing is providing informative perspectives for designers about specific products and let them understand how products impress the customers and how a decision is made to select a product. Therefore, success of advertising a product would be increased and costs of advertising would be optimized.

Neuromarketing investigations performed by using different tools, for example Functional Magnetic Resonance Imaging (fMRI) is a technique that measures the brain's metabolic activity; EEG amplifier is technique that measures brain's electric activity; and eye-tracking technique is employed for considering customers attention and focus [3]. In particular, the fMRI technique is an expensive approach with measurement ability of high spatial resolution (3 mm for the moment) and low temporal resolution (1-3 s for the moment); EEG technique is an affordable approach with high temporal resolution in the measurements which is an advantage [4]; and eye-tracking is a technique that examine the participants eyes pupil's location, but the obtained recent results found it an unreliable method for the neuromarketing studies. Therefore, a numerous neuromarketing studies has been performed by using the EEG signal processing. Here, a selection of related studies to our investigation is presented.

One of the initial neuromarketing studies performed by Vecchiato *et al*. [5] that focused on finding relative EEG frequency bands in a Like/Dislike commercial video clip task. Authors quantified the decision-making procedure (for Like/Dislike selection) by using power spectral density (PSD) brain maps for the theta bands as well as alpha bands. In addition, a correlation analysis applied on the PSDs of the brain maps. Results showed an asymmetrical increase for the theta and alpha amplitudes in different hemispheres when subjects had chosen the pleasant and unpleasant advertisements.

Afterwards, Khushaba *et al*. [6] studied subjects preferences to select a product by using the PSD analysis of brain waves. The spectral activity results showed that the participants preferences affected the frontal (F3 and F4), parietal (P7 and P8), and occipital (O1 and O2) areas. The same team in a series of studies, Khushaba *et al*. [7] employed a different task for visual stimulation to consider the subjects preferences again. The obtained results based on the PSD features showed significant changes in the following regions: frontal region (delta, alpha, and beta across F3, F4, Fc5, and Fc6), temporal region (alpha, beta, gamma across T7), and occipital region (theta, alpha, and beta across O1). Later on, Korkmaz *et al*. [8] used frequency contents for determination of the most discriminative channels and frequencies in a Like/Dislike neuromarketing study. Results showed that the frequency bands of 4 Hz and 5 Hz were determined as the most discriminative ranges in the left frontal (F7) and right temporal (T6) regions.

In a different study, Ramsoy *et al*. [9] performed a neuromarketing investigation of the mechanisms of customers decision-making for willing to pay for a product. In the procedure, the alpha, beta, and gamma frequencies of EEG signal were considered. Statistical analysis showed that the prefrontal gamma asymmetry was related to willing to pay responses significantly. Then, Golnar-Nik *et al*. [10] considered the hypothesis if the PSD feature from the EEG is a suitable approach for predicting the customers decision-making in a Like/Dislike task. In the paper the features were classified by using Support Vector Machine (SVM) and Linear Discriminant Analysis (LDA). Additionally, authors considered the customers preferences in an advertisement task with respect to the background colors of products. Statistical analysis based on the PSD showed the same results as in [9]. In summary, the obtained locations relative to the willing to buying for a product (Like/Dislike tasks) were Centro-parietal locations, namely Fp1, Cp3 and Cpz. In addition, significant changes were observed in the frontal electrodes, namely F4 and Ft8.

Aldayel *et al*. [11] considered customers preferences using EEG signals. In the algorithm, the PSD and valence features were extracted from the filtered EEG signals and then fed into four different classifiers, named deep learning, SVM, Random Forest (RF), and k-Nearest Neighbor (KNN), that the deep learning provided the best accuracy and precision results. Additionally, results showed that the RF classifier obtained similar results as in the deep learning method. The advantage of the deep learning method is the higher potential of producing more accurate and precise results for multi-class identifications problems than the RF and SVM classifiers. Also, deep learning has capability of handling a large number of data, which has been applied on a wide range of different biosignal processing in health monitoring and brain computer interface fields [12], [13]. The disadvantage of the deep learning algorithm is a large number of input data is required for the training phase. Additionally, the training phase is very time consuming process.

In another study, Meyerding *et al*. [14] focused on the neuronal activation of brain during decision-making of label brands for different products. In the algorithm, the difference of neurons activities in the prefrontal cortex (PFC) were measured during subjects coping with two labels brands. The achievements based on the fNIRS showed that the PFC activity for individual subjects increased significantly. The main limitation of the study was participating a low number of subjects in the experiment.

Most recent neuromarketing studies focused on the combination of subjects, while gender is an important parameter which has not been taken into account in the investigations. The primary functions of human's perception is various for different genders points of view and it would be an impressive parameter for improving the neuromarketing models, which has not been considered yet. In addition, linear features are exhaustively studied in the computational parts and a lack of nonlinear feature investigation exists. Table. 1 present a review of some experimental neuromarketing studies.

The first contribution of the present study is identifying the most discriminative areas of brain in a Like/Dislike (willing to buy) task with respect to the subject's gender as an important factor. The second contribution is considering the EEG

TABLE 1. EEG-based neuromarketing studies for assesing the customer preference.

Year	Reference	Number of Subjects	Class	Feature Extraction Selection	Classification Algorithm
2013	[8]	15 (10 females and 5 males)	1. Like 2. Dislike	Power spectral density	-
2016	[15]	5 (3 females and 2 males)	1. Like 2. Dislike	Time-frequency analysis Frequency domain: Power spectral density, Band power, Spectrum power	SVM, KNN
2017	[16]	40 (25 males and 15 females)	1. Like 2. Dislike	Wavelet analysis	ANN (2 layers + Sigmoid), SVM, RF, HMM
2018	[17]	33 (13 males and 20 female)	1. Most favored 2. Least favored	Power	SVM, KNN, Logistic Regression, Decision trees
2019	[10]	16 (9 males and 7 females)	1. Like 2. Dislike 3. Buy	Power	SVM, LDA
2020	[11]	32	1. Like 2. Dislike	Power spectral density, Valence	DNN, KNN, SVM, RF
2021	[18]	25	1. Like 2. Dislike	Spectral energy	Ensemble Classifier, DNN
2022	[19]	20	1. Positive affective attitude 2. Negative affective attitude	Time, Frequency, and Time-frequency	SVM

frequency bands in the determined regions and investigating linear and nonlinear features for identifying Like/Dislike conditions by using the RF, SVM, LDA, and KNN classifiers with respect to the gender of participants. The Like/Dislike decision-making interpreting as a willing to pay for a product or not. The employed features included as follows: PSD and energy of wavelet coefficients, fractal dimension, entropy, and trajectory volume behavior quantifiers. The rest of paper is presented as follows: Section II is the experimental setup and data acquisition; Section III is mathematical methods; Section IV is the results and discussion; and section V is the conclusion.

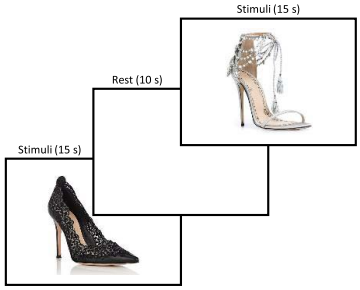

FIGURE 1. The employed structure of experimental protocol in the experiment.

II. EXPERIMENTAL SETUP

The EEG signals recorded from twenty (10 males and 10 females) healthy and graduated right-handed students. Before the experiment, the required regulations and conditions for the task were explained to the subjects and a consent of participation was signed. Participants had no history of neurological or psychiatric disorders as well as no record of medication, alcohol, and drugs consumption. Subjects were recommended not to use caffeinated and nicotine substances for at least four hours before the experiment. The experimental procedure was approved by the national ethics committee in biomedical research.

During the EEG signal recording, subjects should sat on a comfortable chair in a dimly lit room. A set of stimulus images were displayed for the subjects. The images consisted of 16 women's shoes with different styles and colors. Each image displayed 15 seconds on a screen which is located at a distance of one meter. To choose one pairs of shoes, an assigned key should be pressed by the subjects for like (willing to pay) the shoes or another assigned key should be pressed for dislike the shoes (not willing to pay). In the task, a ten second interval rest between displaying images (shoes) was set. The time responses were recorded for the further process. The displayed pictures were women shoes and the main question for women was are you willing to pay for the shoes for herself and male subjects should answer to the question are you willing to pay for the shoes for your life partner (wife). Paradigm blocks were used to display images in the MATLAB software simulation environment. The structure of experimental protocol is shown in Fig. 1.

A. DATA ACQUISITION

A 16-channel EEG amplifier (g.USBamp, g.tec, Austria) was used to record electrical potential. The EEG electrodes were installed based on the international 10-20 electrode location system, in which enable us to cover almost all areas of a head. The main purpose of the 10-20 standard is providing electrode instalment using a small number of electrodes (typically 21 electrodes) for recording EEG. In our experiment, the right ear and Fpz electrodes were set as the GROUND (GND) and common reference for all the channels, respectively. Our electrode instalment is showed in Fig. 2. The EEG was recorded with the sampling frequency of 256 Hz, and a High-pass filter with a cut off frequency of 0.1 Hz and a notch filter with a cut off frequency of 50 Hz were applied. Table. 2 shows the number of decisions for subjects. After collecting the EEG data, the preprocessing method is applied to remove noise.

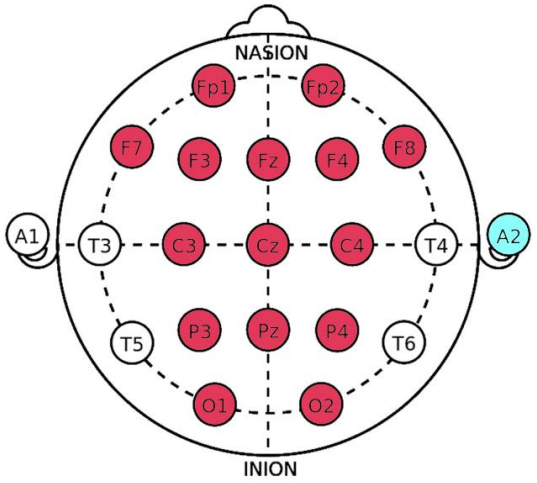

FIGURE 2. Representation of 10-20 system for electrode placement.

TABLE 2. Number of "Like" and "Dislike" decisions for male and female subjects.

	Number of decisions	
	Like	Dislike
Male	71	89
Female	83	77
Total	154	166

III. MATHEMATICAL METHODS

Here, the employed mathematical methods for analysing the EEG signals are presented.The procedure of data analysis is shown in Fig. 3. The first step to process the EEG signal is preprocessing.

A. PREPROCESSING

EEG signals are susceptible to be contaminated easily with physiological and environmental artifacts. To remove noises, the related EEG segments to the decision-making events (Like/Dislike) were extracted. Then, different denoising algorithms were applied to the segments, namely Artifact Subspace Reconstruction (ASR) and Independent Component Analysis (ICA). The main advantage of above-mentioned denoising methods is well-handling physiological artifacts with less signal alterations in comparison with the frequency-based filters. The concept of ASR and ICA methods are presented as follows:

1) ARTIFACT SUBSPACE RECONSTRUCTION

The first noise removal step was employing an ASR method. ASR is one of the automatic artifact removal methods, which is proposed by Kothe *et al.* [20]. The ASR is an effective component-based algorithm for removing transient artifacts in a real-time system [21]. In our algorithm, to remove noise components we employed the well-known ICA method after applying the noise removal ASR technique.

2) INDEPENDENT COMPONENT ANALYSIS

In the second noise removal step, an ICA algorithm applied on the denoised signal. The basic hypothesis concept of ICA is the EEG signal is weighted by using linear combination of electrical potentials, which are generated from independent brain sources [22], [23]. The goal of ICA algorithm is finding the least Gaussian state in a new space in which leads to the identification of the main sources. The ICA is not able to separate the sources of noises if they are completely Gaussian. If the computed components were not independent, then the ICA seek for the most independent space to separate linear sources [24]. Therefore, we mapped the EEG data from the sensor space into the source space and removed the major interference sources including eye components, muscle components, heart components, as well as line noise, and channel noise [25].

B. FEATURE EXTRACTION

To identify the active brain regions in our marketing stimulus experiments, different linear and nonlinear features from five different frequency bands were extracted and analyzed. These analysis were applied on three groups with respect to the genders (male, female, and a combination of male and female). To this end, two sets of linear and nonlinear features were extracted from the EEG signals.

1) LINEAR FEATURE EXTRACTION

The linear feature extraction approaches include the energy of wavelet coefficients and PSD. To this end, the EEG signals were decomposed by using the Discrete Wavelet Transform (DWT) algorithm to obtain different frequency bands. Therefore, a mother wavelet is set in the DWT, named Daubechies 8 (db8) and then the DWT was applied for five levels to reach the aim frequency bands [26], [27]. The energy of DWT coefficients were computed as follows:

$$E_i = \sum_{i=1}^{N} C_i, j^2, \tag{1}$$

where C_i, j represents i-th coefficient of j-band and N is the number of j-band coefficients.

The PSD feature computed by means of modified periodogram algorithm, which is a non-parametric estimation. The PSD algorithm involves following steps: 1) multiplying the input time series with a non-rectangular window such as Hamming; 2) applying the Fourier transform function; and 3) computing the density of power spectrum estimation by using the Fourier transform size. Typically, the non-parametric methods have less computational complexity than the parametric models. Therefore, the PSD features were extracted from the frequency bands consist of Delta (0.5-4 Hz), Theta (4-8 Hz), Alpha (8-13 Hz), Beta (13-30 Hz), and Gamma (30-40 Hz). In the computations, there was no restriction for selecting the frequency bands.

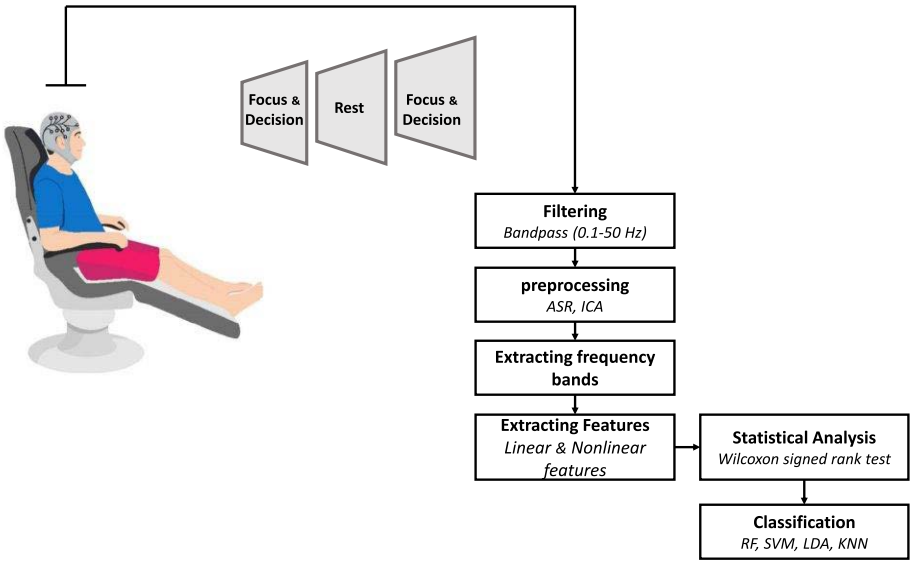

FIGURE 3. Procedure of data analysis of the proposed system.

2) NONLINEAR FEATURE EXTRACTION

Brain function is a non-stationary system that produces signals with high level of complexity [28]. Since now several methods has been developed to interpret the brain neurons activities which are recorded by the EEG. One approach to study the dynamics of a nonlinear system is investigating the chaotic behavior of a system [29]. The chaotic methods apply techniques for quantifying the nonlinear features of a system such as quantification of trajectory volume behavior, entropy, and fractal dimensions [26].

The idea of entropy was first proposed in the thermodynamic field to measure the trajectory of a system. The entropy concept describes the behavior of a part of a trajectory that can be predicted from the rest. In the computations, the higher entropy in a system leads to higher complexity, which means less chance for predicting the systems behaviour [30], [31]. In the present study, we have employed different features based on the entropy computations, namely spectral entropy, approximation entropy, and sample entropy.

The second set of our chaotic features for measuring the complexity of an EEG was fractal dimensions. The fractal dimension concept is a numerical scale method for measuring how much space is filled by a pattern. The hallmark characteristics of fractals that we make use of them are self-similarity and non-integer dimension. In our computations, Higuchi and Katz fractal dimensions were employed [31].

The third set of chaotic features is the trajectory of EEG signals in a reconstructed phase space, which is computed using two delayed EEG signals [29]. The obtained chaotic-based quantifiers quantify the volumetric behavior of a trajectory in a phase space. The basis of computations is the expansion and compaction of a trajectory. For this purpose, the features in [32] study are implemented.

According to the Taken's theory [33], growing the trajectory of EEG signals in a reconstructed phase space is applicable using the time series $X(t) = \{x_1, x_2, \ldots, x_N\}$ and two delayed input signals as follows [34], [35]:

$$\overrightarrow{X}_i(t) = (x_i, x_{i+\tau}, \ldots, x_{i+(\mu-1)\tau}) \quad i = [1 \quad N - (\mu - 1)\tau] \tag{2}$$

where μ and τ are embedding dimension and delay, respectively, which are obtained based on the false nearest-neighbors and mutual information methods. To extract features, the Euclidean distance matrices (T) of trajectories (L) with length N between all the state vectors are computed follows:

$$L = \overrightarrow{X}_1, \overrightarrow{X}_2, \ldots, \overrightarrow{X}_N. \tag{3}$$

Matrix T' is obtained by removing the main diagonal of matrix T. The last column of the matrix T' is then removed and shifted to the left. Matrix T'' with dimension $(M \times (M - 2))$ represents the difference between the distances of state vectors and trajectory motion.

Regarding the trajectory of EEG signals in the reconstructed phase space several features extracted, namely Occupational Size (OS), Average Expansion Speed (AES), Average Compression Speed (ACS), Average Expansion (AE), Average Compression (AC), Standard Deviation Expansion Speed (SDES), Standard Deviation Compression Speed (SDCS), and Complexity. The above-mentioned feature definitions are as follows:

- OS: The average across all elements in matrix T.
- AES: The average of negative numbers in matrix T''.
- ACS: The average of positive numbers in matrix T''.
- AE: The normalized expansion rate.
- AC: The normalized compression rate.

- SDES: Variation of negative numbers in matrix T''.
- SDCS: Variation of positive numbers in matrix T''.
- Complexity: Summation of number of the positive elements in SDCS (T'') and the number of negative elements in SDES (T'') after normalization.

The computed features are analyzed to find the most discriminative channels and frequency bands between the Like/Dislike groups. To evaluate the separability of features, the Wilcoxon Rank Sum statistical test is applied, which is explained in the next step.

C. STATISTICAL ANALYSIS

The Wilcoxon Rank Sum statistical analysis is a non-parametric test that examines the difference of a measurement quantity between two groups whose samples are independent from each other. This test is based on the median comparison. In this research, the Wilcoxon Rank Sum statistical analysis was applied for recognition of the discriminative channels in five frequency bands. The obtained features distribution was not Gaussian and it satisfies the Wilcoxon Rank Sum's assumptions. We used the MATLAB statistical analysis toolbox for the computations. In our experiment, the statistical analysis between the difference of Like/Dislike groups found significant. The determined significant features are then employed for identifying the Like/Dislike conditions by using RF, SVM, LDA, and KNN classifiers. SVM and LDA are the most common metrics used by most research in the domain of customer preferences for evaluation. More than half of the EEG-based papers have used them [11]. According to reference [11], deep learning has similar results to RF. So, we used Random Forest rather than DNN due to the limited number of subjects.

D. CLASSIFICATION

To classify the Like/Dislike conditions several studies have been employed by using linear features. In addition, we have extracted discriminative frequency bands by using classification. Here, we employed the well-known RF, SVM, LDA, and KNN classifiers to identify the Like/Dislike conditions by using linear and nonlinear features.

1) RF CLASSIFIER

RF is a statistical method for supervised learning classification, which was introduced by Leo Breiman [36]. The RF makes several decision trees and merges them together to make a more accurate and stable prediction. The RF classifier generates trees randomly to generate forests. The greater the number of trees, the more accurate estimation. Therefore, it is concluded that a meaningful relation between the number of trees in the RF algorithm and the obtained results exists [37]. Shortly, the RF contains multiple decision trees that each decision tree considers a set of data. The final RF classification decision is made based on the previous decisions in the trees. The advantages of RF algorithm is reducing the probability of overfitting and high variance in comparison with decision tree algorithms. The second classifier is SVM method.

2) SVM CLASSIFIER

SVM is a supervised learning classifier, which is based on statistical learning theory. The first nonlinear SVM model introduced by Vapnik [38]. Conceptually, the SVM model is a hyperplane or line that separates a set of positive and negative samples, namely support vectors, by using a maximum distance [39], [40]. Recently, several modifications of the SVM has been developed to increase the accuracy and precision results [41], [42]. In the computations, the boundaries of the two classes may not be linearly separable. Therefore, features are mapped from the input space to a feature space with higher dimension by means of nonlinear kernels. The mapped feature space dimension is increased until the features are separable linearly [43]. Different types of kernels has been employed for the SVM decision function, the most common used kernel in the SVM algorithm is the Radial Basis Function (RBF). The advantages of RBF are using Gaussian shape for the distributions and enabling a feature space with unlimited dimensions [44]. Also, several method developed to improve the capability of RBF [41], [45].

3) LDA CLASSIFIER

LDA is a linear model commonly used for supervised classification problems and dimensionality reduction. This technique offer a good separation between different classes and avoid overfitting. As a result, computational costs will be significantly reduced and classification will be more accurate by projecting the given n-dimensional feature space onto a smaller feature space while maximizing the class separability [46].

4) KNN CLASSIFIER

KNN is a non-parametric and supervised learning algorithm. This algorithm is simple to implement and robust to the noisy training data which can be used for both classification and regression. In KNN, inputs are classified based on their K neighbors. The disadvantage of the algorithm is the value of K will always need to be determined, which may be complicated. Since the distance between the data points for all the samples of training dataset must be calculated, the computation cost will be high. In the next step, the obtained results are presented and discussed.

IV. RESULT AND DISCUSSION

In the present study, 20 subjects participated in the experiment and EEG signals were recorded by using visual Like/Dislike stimulation task. The above-mentioned algorithms were then applied on the EEG data to find the distinctive frequency bands and the relative areas of brain which were affected by willing to pay decision for a pair of shoes. Here, the results of frequency bands, brain regions and the effects of nonlinear and linear features on the distinguished

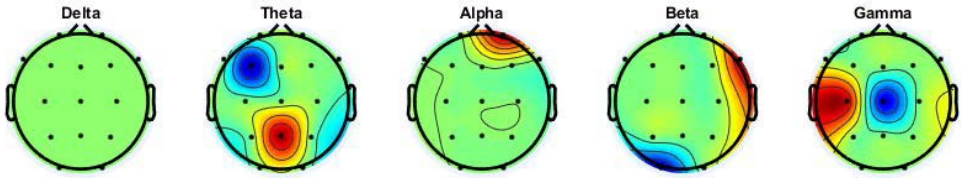

(a) Nonlinear features for female subjects

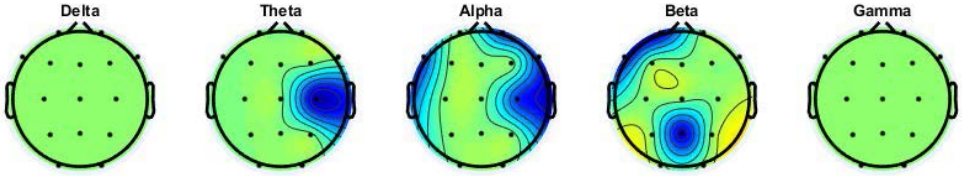

(b) Linear features for female subjects

FIGURE 4. The obtained affected areas of female's brain during displaying images in a Like/Dislike task, by using (a) Nonlinear and (b) linear features.

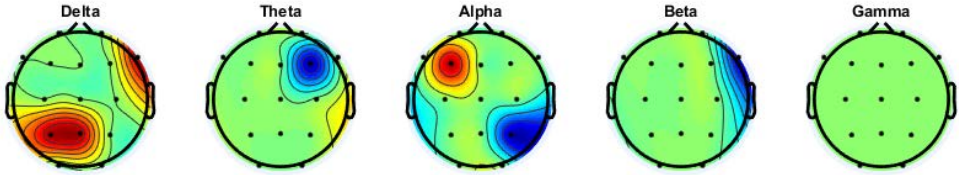

FIGURE 5. The obtained affected areas of male's brain during displaying images in a Like/Dislike task by using nonlinear features.

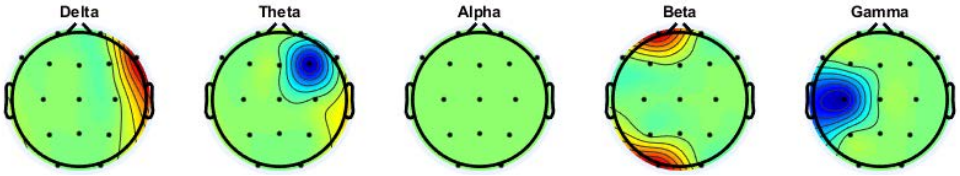

(a) Nonlinear features for the combination of all subjects.

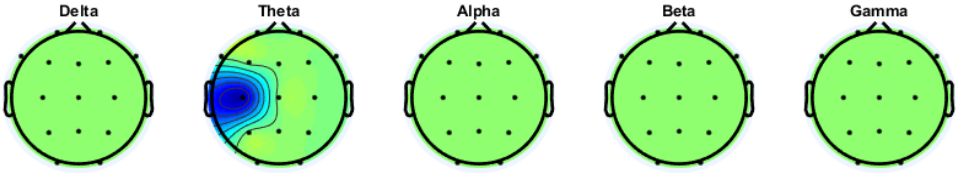

(b) Linear features for the combination of all subjects.

FIGURE 6. The obtained affected areas of all subject's brain during displaying images for a Like/Dislike task, by using (a) nonlinear and (b) linear features.

brain regions are analyzed with respect to the gender of subjects.

A. STATISTICAL ANALYSIS OF LINEAR FEATURES VS. NONLINEAR FEATURES

To investigate how gender influences decision-making, subjects were categorized in three groups to perform a Like/Dislike task. The groups involved 1) males, 2) females and 3) combination of males and females. In addition to using linear features, a set of nonlinear features were employed to compute features. The Wilcoxon Rank Sum statistical analysis was then applied on the explained linear and nonlinear features, which were extracted from the main five frequency bands and then scalp maps were created. The guide line for interpreting scalp maps such as Fig. 4b is as follows: the blue regions shows that the average value of extracted features for the Dislike condition is greater than the Like condition. Additionally, the red regions are the channels where the average value of extracted features for the Like condition is greater than the Dislike condition. The following

TABLE 3. Like/Dislike condition classification by using (a) linear and (b) Nonlinear features for female subjects.

(a) Linear features for female subjects.

Classifier	Metric	Theta	Alpha	Beta	All Bands
RF	Accuracy	55.11 ± 7.19	61.91 ± 5.44	58.31 ± 8.81	63.19 ± 7.02
	Sensitivity	57.76 ± 15.63	65.77 ± 11.53	60.92 ± 9.22	64.21 ± 7.46
	Specificity	53.79 ± 7.71	59.84 ± 11.71	56.55 ± 10.98	62.66 ± 12.1
SVM	Accuracy	65.53 ± 5.84	57.94 ± 3.34	60.81 ± 2.39	71.51 ± 5.10
	Sensitivity	57.18 ± 6.85	55.02 ± 4.51	63.85 ± 7.41	78.19 ± 5.79
	Specificity	74.27 ± 6.72	60.79 ± 6.76	57.75 ± 7.92	64.88 ± 6.16
LDA	Accuracy	61.08 ± 3.73	56.75 ± 0.02	62.44 ± 3.72	62.14 ± 2.17
	Sensitivity	54.45 ± 4.79	51.42 ± 5.69	72.86 ± 6.08	56.20 ± 7.01
	Specificity	67.72 ± 3.88	61.94 ± 2.87	52.17 ± 4.29	67.8 ± 3.94
KNN	Accuracy	60.36 ± 8.73	61.96 ± 3.24	60.03 ± 4.24	61.84 ± 3.95
	Sensitivity	55.23 ± 7.45	63.2 ± 2.94	57.29 ± 3.51	69.4 ± 1.21
	Specificity	65.44 ± 10.72	60.71 ± 5.46	62.75 ± 5.78	$54.7 \pm .58$

(b) Non-Linear features for female subjects.

Classifier	Metric	Theta	Alpha	Beta	Gamma	All Bands
RF	Accuracy	55.53 ± 9.59	57.87 ± 6.41	55.74 ± 10.31	61.87 ± 10.39	60 ± 8.32
	Sensitivity	53.73 ± 16.19	60.19 ± 8.82	52.66 ± 13.27	65.81 ± 10.24	54.28 ± 10.37
	Specificity	57.64 ± 11.66	55.97 ± 8.44	59.94 ± 11.27	59.25 ± 13.47	66.58 ± 11.83
SVM	Accuracy	62.41 ± 4.7	57.79 ± 2.93	59.1 ± 5.64	60.04 ± 2.19	67.42 ± 1.83
	Sensitivity	61.19 ± 8.37	62.47 ± 4.98	61.47 ± 3.64	58.91 ± 5.45	62.19 ± 4.54
	Specificity	63.77 ± 2.76	53.2 ± 5.07	58.48 ± 12.38	71.37 ± 4.14	72.68 ± 5.94
LDA	Accuracy	66.84 ± 3.39	62.49 ± 1.88	64.18 ± 4.34	62.22 ± 4.53	65.51 ± 3.81
	Sensitivity	68.11 ± 3.49	60.83 ± 3.81	67.95 ± 12.1	64.14 ± 3.44	66.99 ± 4.59
	Specificity	65.56 ± 4.61	64.11 ± 2.09	60.38 ± 4.21	60.11 ± 10.47	64.13 ± 6.27
KNN	Accuracy	56.99 ± 2.88	61.36 ± 4.23	56.26 ± 6.83	66.59 ± 10.22	61.71 ± 3.3
	Sensitivity	51.46 ± 2.08	62.68 ± 9.13	62.99 ± 7.49	65.15 ± 10.38	62.35 ± 4.02
	Specificity	62.47 ± 6.91	59.83 ± 7.16	49.25 ± 6.21	68.08 ± 10.5	61.33 ± 9.21

TABLE 4. Like/Dislike condition classification by using nonlinear features for male subjects.

Classifier	Metric	Delta	Theta	Alpha	Beta	All Bands
RF	Accuracy	58.14 ± 6.93	53.49 ± 5.4	53.95 ± 6.18	52.09 ± 8.14	71.33 ± 14.07
	Sensitivity	52.72 ± 12.3	65 ± 6.1	50.57 ± 10.36	48.82 ± 13.46	70.7 ± 9.08
	Specificity	62.8 ± 9.1	60.01 ± 9.7	58.23 ± 7.05	57.09 ± 14.71	65.22 ± 10.39
SVM	Accuracy	66.44 ± 4.07	60.30 ± 4.68	52.94 ± 5.68	62.34 ± 3.57	63.12 ± 3.01
	Sensitivity	68.99 ± 10.72	59.17 ± 7.99	57.04 ± 12.96	71.33 ± 5.53	59.71 ± 2.58
	Specificity	63.92 ± 7.65	65.39 ± 5.29	53.76 ± 5.72	59.27 ± 4.93	77.03 ± 4.89
LDA	Accuracy	63.64 ± 2.05	60.36 ± 2.06	59.72 ± 2.12	65.74 ± 6.07	63.65 ± 4.41
	Sensitivity	70.55 ± 3.97	59.61 ± 5.04	64.07 ± 3.69	73.52 ± 7.92	66.89 ± 7.54
	Specificity	57.01 ± 3.56	61.08 ± 8.56	55.38 ± 2.06	57.97 ± 6.13	60.41 ± 4.28
KNN	Accuracy	61.71 ± 2.36	52.38 ± 5.83	52.41 ± 2.36	55.16 ± 3.95	66.49 ± 4.63
	Sensitivity	63.53 ± 4.21	49.72 ± 2.81	44.11 ± 3.49	58.11 ± 3.73	57.17 ± 1.72
	Specificity	59.88 ± 3.48	55.04 ± 13.33	60.78 ± 6.81	52.15 ± 5.98	75.83 ± 9.04

parts are analyzing the obtained results in three parts (significant features, channels and frequency ranges) for each group.

1) Consideration of female group: Fig. 4a demonstrates the discriminative channels and frequency bands based on nonlinear features between Like/Dislike conditions. It is evident that the activated frequency bands and regions underlying of Like condition (willing to pay) are as follows (average *Like* $>$ *Dislike*): the theta band in parietal (Pz) region; the alpha band in right prefrontal (Fp2) region; the beta band in right frontal (F8) region; and the gamma band in left central (C3) region. Additionally, the activated frequency bands and regions underlying of Dislike condition (not willing to pay) are as follows (average *Dislike* $>$ *Like*): the theta band in left frontal (F3) region; the beta band in left occipital (O1) region; and the gamma band in central (Cz) region. Fig. 4a shows non-distinctive changes by using the nonlinear features from the delta band between Like/Dislike classes.

Fig. 4b demonstrates the discriminative channels and frequency bands based on the linear features between Like/Dislike conditions. It is evident that the average of Dislike condition was stronger than the Like condition (blue regions - average *Dislike* $>$ *Like*). The affected frequency bands and regions for the Dislike condition are as follows: the theta band in right central (C4) region; the alpha band in frontal (F7, F8, Fp2) and right central (C4) regions; the beta band in left frontal (Fp1, F7) and parietal (Pz) regions. No region was affected under Like condition by using the linear features. Results showed insignificant changes in the delta and gamma bands.

TABLE 5. Like/Dislike condition classification by using (a) linear and (b) nonlinear features for combined male and female subjects.

(a) Linear features for combined male and female subjects.

Classifier	Metric	Theta	All Bands
RF	Accuracy	62.25 ± 8.05	62.25 ± 8.05
	Sensitivity	63.96 ± 14.08	63.96 ± 14.08
	Specificity	60.14 ± 11.24	60.14 ± 11.24
SVM	Accuracy	57.29 ± 1.6	57.29 ± 1.6
	Sensitivity	53.33 ± 3	53.33 ± 3
	Specificity	81.01 ± 0.75	81.01 ± 0.75
LDA	Accuracy	54.93 ± 2.7	54.93 ± 2.7
	Sensitivity	53.15 ± 4.41	53.15 ± 4.41
	Specificity	66.55 ± 2.32	66.55 ± 2.32
KNN	Accuracy	68.26 ± 1.8	68.26 ± 1.8
	Sensitivity	64.02 ± 6.22	64.02 ± 6.22
	Specificity	72.35 ± 6.46	72.35 ± 6.46

(b) Nonlinear features for combined male and female subjects.

Classifier	Metric	Delta	Theta	Beta	Gamma	All Bands
RF	Accuracy	52.58 ± 6.98	50.32 ± 5.08	63.22 ± 5.93	50.32 ± 9.02	65.16 ± 6.78
	Sensitivity	57.27 ± 15.53	51.53 ± 8.38	58.82 ± 9.83	53.95 ± 12.93	64.55 ± 10.12
	Specificity	49.77 ± 13.63	49.96 ± 10.8	67.35 ± 8.21	50.22 ± 13.01	66.51 ± 14.64
SVM	Accuracy	60.21 ± 3.86	60.18 ± 2.84	62.52 ± 1.78	60.29 ± 3.09	61.52 ± 3.83
	Sensitivity	65.59 ± 3.22	67.52 ± 5.33	64.17 ± 6.81	45.04 ± 3.16	62.69 ± 2.38
	Specificity	54.85 ± 5.21	52.91 ± 2.11	60.75 ± 5.78	75.65 ± 3.77	60.36 ± 5.56
LDA	Accuracy	59.83 ± 1.69	58.59 ± 2.29	59.78 ± 2.31	55.67 ± 1.53	57.4 ± 3.68
	Sensitivity	59.48 ± 3.47	66.07 ± 3.49	59.7 ± 5.14	61.74 ± 2.29	58.61 ± 2.43
	Specificity	60.18 ± 1.27	51.29 ± 2.79	59.1 ± 8.91	49.69 ± 2.1	56.22 ± 5.24
KNN	Accuracy	52.9 ± 3.62	48.06 ± 4.74	51.28 ± 6.57	52.19 ± 2.91	56.21 ± 2.36
	Sensitivity	48.32 ± 3.23	46.96 ± 3.24	50.09 ± 7.01	50.98 ± 3.89	56.77 ± 2.16
	Specificity	57.3 ± 9.04	49.1 ± 7.37	52.46 ± 6.8	53.4 ± 2.69	55.65 ± 2.81

2) Consideration of male group: Fig. 5 demonstrates the discriminative channels and frequency bands based on nonlinear features between Like/Dislike conditions. It is evident that the activated frequency bands and regions underlying of Like condition (willing to pay) are as follows (average *Like* > *Dislike*): the delta band in right frontal (F8), left parietal (P3) and central parietal (Pz) regions; and the alpha band in left frontal (F3). In addition, the activated frequency bands and regions underlying of Dislike condition (not willing to pay) are as follows (average *Dislike* > *like*): the theta band in right frontal (F4) region; the alpha band in right parietal (P4) region; and the beta band in right frontal (F8) region. Moreover, results showed that the extracted linear features from the delta, theta, alpha, beta, and gamma frequency bands for identifying the Like/Dislike conditions were insignificant. As it is evident, the nonlinear features has potential of carrying information from the EEG which are not visible by using the linear attribute features.

3) Combination of male and female groups: Fig. 6a demonstrates the discriminative channels and frequency bands based on nonlinear features between Like/Dislike conditions. It is evident that the activated frequency bands and regions underlying of Like condition (willing to pay) are as follows (average *Like* > *Dislike*): the delta band in right frontal (F8) region; the beta band in left prefrontal (Fp1) and left occipital (O1) regions. In addition, the activated frequency bands and regions underlying of Dislike condition (not willing to pay) are as follows (average *Dislike* > *like*): the theta band in right frontal (F4) region; and the gamma band in left central (C3) region. For all subjects, the alpha band changes between Like/Dislike conditions was insignificant.

Fig. 6b demonstrates distinctive regions in all frequency bands based on the linear features between Like/Dislike decision-making task. It is evident that the average of Dislike condition was stronger than the Like condition. The significant results for Dislike condition were obtained from the theta band in left central (C3) region. The obtained results based on the nonlinear features showed insignificant differences in the delta, alpha, beta, and gamma frequency bands between Like/Dislike conditions.

B. LIKE/DISLIKE CLASSIFICATION PERFORMANCE

To identify the discriminated frequency bands between Like/Dislike groups, well-established RF, SVM, LDA, and KNN classifiers were employed. In the process, a matrix size of $15 \times 14 \times 160$ was formed for individual subjects, i.e., 15 channels, 14 features, and 16 Like/Dislike epochs. In our study, the reported accuracy results for the Like/Dislike classification are based on a 10-fold cross-validation. The explanations are performed based on the genders.

Performance of female group classification: Table. 3a illustrates the performance of the Like/Dislike conditions identification based on the linear features. According to the RF, SVM, LDA, and KNN classifiers results, the SVM classifier achieved the highest accuracy of $71.51 \pm 5.10\%$. In the algorithm, the most informative revealed extracted feature was the energy of wavelet coefficient from the combination

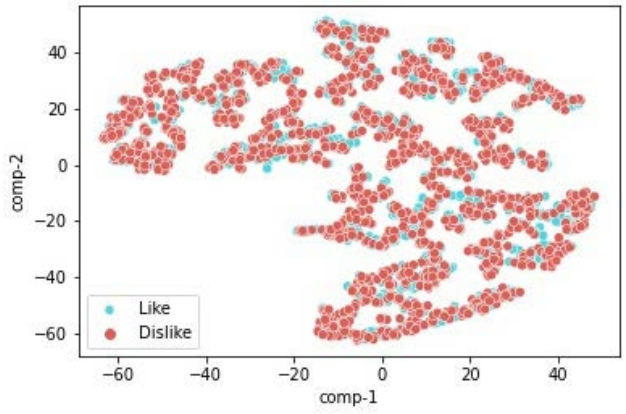

(a) Delta frequency band t-SNE projection.

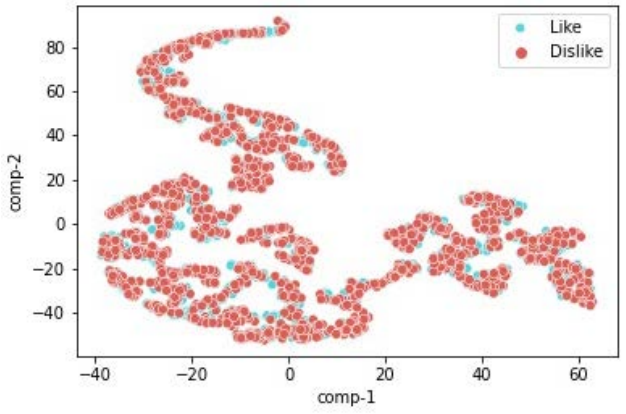

(b) Theta frequency band t-SNE projection.

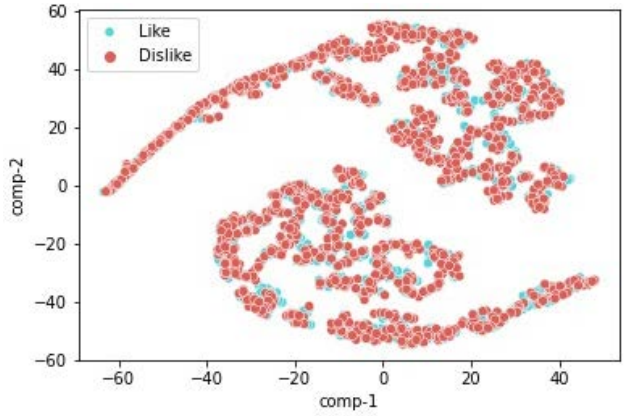

(c) Alpha frequency band t-SNE projection.

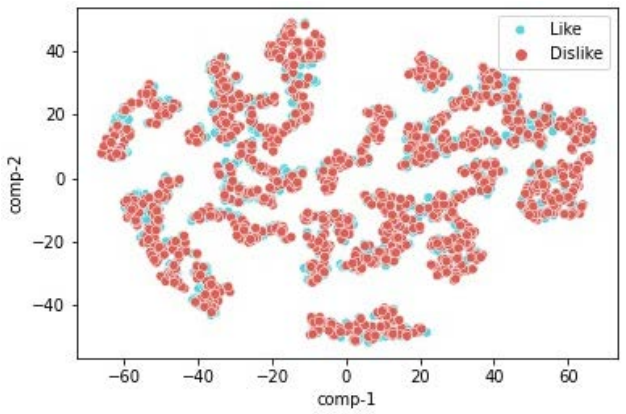

(d) Beta frequency band t-SNE projection.

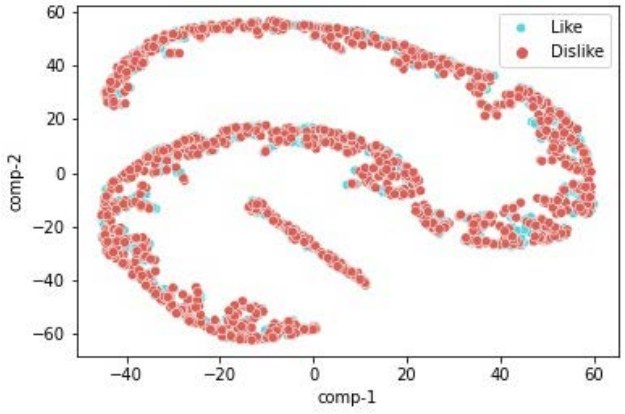

(e) Gamma frequency band t-SNE projection.

FIGURE 7. Distribution of linear features in different frequency bands (a) Delta, (b) Theta, (C) Alpha, (d) Beta, and (e) Gamma in a Like/Dislike task for male subjects.

of theta, alpha, and beta frequency bands in channels Fp1, Fp2, F7, F8, Cz, and Pz. Table. 3b illustrates the results of Like/Dislike conditions identification based on the nonlinear features. Results illustrated that the SVM classifier achieved the highest accuracy rate of 67.42 $\pm$ 1.83%. In the algorithm, the most informative revealed extracted features were the spectral entropy features, katz, higuchi fractal dimension, ACS, AES, AC, AE, SDCS, and SDES from the combination of theta, alpha, beta, and gamma frequency bands in channels Fp2, F3, F8, C3, Cz, Pz, and O1. The reason for higher outcome for the selected nonlinear features is a wider scattering with less overlap in the feature space that this in turn could provide more accurate result. As a consequence of this advantage, a lower

number of dimensions is required to be applied to obtain the best accuracy, which means faster and less complicated processing.

Performance of male group classification: Table. 4 illustrates the performance of Like/Dislike conditions identification based on the nonlinear features. In the algorithm, the most informative revealed extracted features were the sample entropy, approximate entropy, and the Higuchi fractal dimension from the combination of delta, theta, alpha, and beta frequency bands in channels F3, F4, F8, P3, P4, and Pz. The RF classifier achieved the best accuracy rate of $71.33 \pm 14.07\%$ using nonlinear features.

Performance of combination of male and female group: Table. 5a illustrates the performance of Like/Dislike conditions identification based on the linear features. In the algorithm, the most informative revealed extracted feature was the PSD feature from the theta frequency band in channel C3. The KNN classifier achieved the best accuracy rate of $68.26 \pm 1.8\%$ using the linear features. Table. 5b illustrates the performance of Like/Dislike conditions identification based on the nonlinear features. In the algorithm, the most informative revealed extracted features were sample entropy, approximation entropy, Katz, and Higuchi fractal dimensions from the delta, theta, beta, and gamma frequency bands in channels Fp1, F4, F8, C3, and O1. The RF classifier achieved the accuracy rate of $65.16 \pm 6.78\%$ in comparison with the RF classifier using the nonlinear features. In this case, the chaotic features attain our objective in identifying Like/Dislike task with significant accuracy result.

Most of studies are based on the combination of genders in one group that the achieved results for the third group in the our study are different from the previous studies. Specifically, we found that the theta frequency band in central (C3) region was found the most discriminative channel. Additionally, the linear features with the KNN classifier reach the highest accuracy rate of $68.26 \pm 1.8\%$. While, Golnar-Nik *et al.*] [10] showed that the accuracy rate for identifying Like/Dislike preferences was 63.00%. In another study, Pereira *et al.* [47] showed that the frontal lobe were activated in a Like/Dislike music task, whilst in our study the region was central (C3) region. Also, Andersen and Cui [48] showed that the frontal area and parietal regions were interconnected for several factors of decision-making. The incremental accuracy achievements using the nonlinear features in the three groups could be attributable to the complexity of EEG signals.

In our study, we also considered the required average time for performing the Like/Dislike task that for the three groups it was approximately 2.5 seconds, which is in good agreement with the studies conducted by Witchalls [49]. Additionally, We found Dislike decision-making happens a little later than Like, more specifically the Like decision-making took place in 2.2 ± 0.003 second and Dislike decision-making took place in 2.6 ± 0.02 second. Our experiments showed that there are several human protocols for different types of subjects, which are missed in the computations. In future research, we will increase the number of subjects and improve the accuracy by using improving the mathematical methods of classification.

In summary, the identification of disctinctive frequency bands, brain regions and Like/Dislike conditions are highly depend on linear and nonlinear features. According to the female investigation achievements it is evident that the most discriminative frequency for the females was the combination of theta, alpha, and beta frequency bands in frontal (Fp1, Fp2, F7, F8), central (Cz), and parietal (Pz) regions. In the classification part, by making use of the energy of wavelet coefficient feature with the SVM classifier the females group achieved the best accuracy of $71.51 \pm 5.10\%$ for Like/Dislike identification. For male group, linear features extracted from the delta, theta, alpha, beta, and gamma frequency bands were insignificant in identifying Like/Dislike conditions, as Fig. 7 shows.

According to the male group, it is evident that the most discriminative frequency was the combination of delta, theta, alpha and beta bands in frontal (F3, F4, F8) and parietal (P3, P4, Pz) regions. In the classification part, by making use of the sample entropy, approximation entropy and Higuchi fractal dimension features and RF classifier the male group reach the best accuracy of $71.33 \pm 14.07\%$ for Like/Dislike identification. Finally, according to the the combined group, it is evident that the most discriminative frequency band was the theta in central (C3) region. In the classification part, by making use of the linear features and KNN classifier the combined female and male groups reach the best accuracy of $68.26 \pm 1.8\%$ for Like/Dislike identification.

V. CONCLUSION

In the present study, a neuromarketing experimental task by using the EEG amplifier was designed to display image of shoe products for males and females. Brain regions related to the decision-making procedure of Like/Dislike products were considered for different genders. Therefore, different linear and nonlinear features were extracted from different frequency bands and brain regions. The Wilcoxon Rank Sum statistical test was then applied on the features to specify distinctive frequencies and regions due to visual stimulation task. Additionally, the best linear/nonlinear features for identifying Like/Dislike classes were considered with respect to the genders. The extracted features from the distinctive EEG channels were categorized by using the RF, SVM, LDA, and KNN classifiers. Some part of significant results showed that partially different areas of the brain were activated during Like/Dislike tasks in comparison with other studies for a mixed gender group. In addition, more areas and frequency ranges were activated in female's brain during shopping in comparison with male. The classification results illustrated that the SVM classifier achieved more accurate results in comparison with the other classifier for female groups. Additionally, the combination of frequency bands has potential of achieving more accurate results for identifying Like/Dislike (willing to pay or not) conditions by means of a classifier

in comparison with extracting features from individual frequency bands with the same classifier.

REFERENCES

[1] B. Veronica, "Brief history of neuromarketing," *J. Bert. Rus.*, pp. 119–121, 2009.

[2] B. Y. Ozkara and R. Bagozzi, "The use of event related potentials brain methods in the study of conscious and unconscious consumer decision making processes," *J. Retailing Consum. Services*, vol. 58, Jan. 2021, Art. no. 102202.

[3] M. D. Bercea, "Anatomy of methodologies for measuring consumer behavior in neuromarketing research," in *Proc. LCBR Eur. Marketing Conf.*, 2012, pp. 1–14.

[4] C. Solnais, J. Andreu-Perez, J. Sánchez-Fernández, and J. Andréu-Abela, "The contribution of neuroscience to consumer research: A conceptual framework and empirical review," *J. Econ. Psychol.*, vol. 36, pp. 68–81, Jun. 2013.

[5] G. Vecchiato, J. Toppi, L. Astolfi, F. De Vico Fallani, F. Cincotti, D. Mattia, F. Bez, and F. Babiloni, "Spectral EEG frontal asymmetries correlate with the experienced pleasantness of TV commercial advertisements," *Med. Biol. Eng. Comput.*, vol. 49, no. 5, pp. 579–583, May 2011.

[6] R. N. Khushaba, L. Greenacre, S. Kodagoda, J. Louviere, S. Burke, and G. Dissanayake, "Choice modeling and the brain: A study on the electroencephalogram (EEG) of preferences," *Expert Syst. Appl.*, vol. 39, no. 16, pp. 12378–12388, Nov. 2012.

[7] R. N. Khushaba, C. Wise, S. Kodagoda, J. Louviere, B. E. Kahn, and C. Townsend, "Consumer neuroscience: Assessing the brain response to marketing stimuli using electroencephalogram (EEG) and eye tracking," *Expert Syst. Appl.*, vol. 40, no. 9, pp. 3803–3812, Jul. 2013.

[8] B. Yılmaz, S. Korkmaz, D. B. Arslan, E. Güngör, and M. H. Asyalı, "Like/dislike analysis using EEG: Determination of most discriminative channels and frequencies," *Comput. Methods Programs Biomed.*, vol. 113, no. 2, pp. 705–713, Feb. 2014.

[9] T. Z. Ramsøy, M. Skov, M. K. Christensen, and C. Stahlhut, "Frontal brain asymmetry and willingness to pay," *Frontiers Neurosci.*, vol. 12, p. 138, Mar. 2018.

[10] P. Golnar-Nik, S. Farashi, and M.-S. Safari, "The application of EEG power for the prediction and interpretation of consumer decision-making: A neuromarketing study," *Physiol. Behav.*, vol. 207, pp. 90–98, Aug. 2019.

[11] M. Aldayel, M. Ykhlef, and A. Al-Nafjan, "Deep learning for EEG-based preference classification in neuromarketing," *Appl. Sci.*, vol. 10, no. 4, p. 1525, Feb. 2020.

[12] A. Hekmatmanesh, V. Zhidchenko, K. Kauranen, K. Siitonen, H. Handroos, S. Soutukorva, and A. Kilpelainen, "Biosignals in human factors research for heavy equipment operators: A review of available methods and their feasibility in laboratory and ambulatory studies," *IEEE Access*, vol. 9, pp. 97466–97482, 2021.

[13] A. Hekmatmanesh, P. H. J. Nardelli, and H. Handroos, "Review of the state-of-the-art of brain-controlled vehicles," *IEEE Access*, vol. 9, pp. 110173–110193, 2021.

[14] S. G. H. Meyerding and C. M. Mehlhose, "Can neuromarketing add value to the traditional marketing research? An exemplary experiment with functional near-infrared spectroscopy (fNIRS)," *J. Bus. Res.*, vol. 107, pp. 172–185, Feb. 2020.

[15] L. H. Chew, J. Teo, and J. Mountstephens, "Aesthetic preference recognition of 3D shapes using EEG," *Cognit. Neurodyn.*, vol. 10, no. 2, pp. 165–173, 2016.

[16] M. Yadava, P. Kumar, R. Saini, P. P. Roy, and D. P. Dogra, "Analysis of EEG signals and its application to neuromarketing," *Multimedia Tools Appl.*, vol. 76, no. 18, pp. 19087–19111, 2017.

[17] A. Hakim, S. Klorfeld, T. Sela, D. Friedman, M. Shabat-Simon, and D. J. Levy, "Pathways to consumers' minds: Using machine learning and multiple EEG metrics to increase preference prediction above and beyond traditional measurements," *BioRxiv*, Aug. 2018, Art. no. 317073.

[18] M. Alimardani and M. Kaba, "Deep learning for neuromarketing; classification of user preference using EEG signals," in *Proc. 12th Augmented Hum. Int. Conf.*, May 2021, pp. 1–7.

[19] F. R. Mashrur, K. M. Rahman, M. T. I. Miya, R. Vaidyanathan, S. F. Anwar, F. Sarker, and K. A. Mamun, "BCI-based Consumers' choice prediction from EEG signals: An intelligent neuromarketing framework," *Frontiers Hum. Neurosci.*, vol. 16, May 2022, Art. no. 861270.

[20] C. A. E. Kothe and T.-P. Jung, "Artifact removal techniques with signal reconstruction," U.S. Patent 14 895 440, Apr. 28, 2016.

[21] C.-Y. Chang, S.-H. Hsu, L. Pion-Tonachini, and T.-P. Jung, "Evaluation of artifact subspace reconstruction for automatic EEG artifact removal," in *Proc. 40th Annu. Int. Conf. IEEE Eng. Med. Biol. Soc. (EMBC)*, Jul. 2018, pp. 1242–1245.

[22] S. Makeig, T.-P. Jung, A. J. Bell, D. Ghahremani, and T. J. Sejnowski, "Blind separation of auditory event-related brain responses into independent components," *Proc. Nat. Acad. Sci. USA*, vol. 94, no. 20, pp. 10979–10984, 1997.

[23] A. J. Bell and T. J. Sejnowski, "An information-maximization approach to blind separation and blind deconvolution," *Neural Comput.*, vol. 7, no. 6, pp. 1129–1159, 1995.

[24] A. Hyvärinen and E. Oja, "Independent component analysis: Algorithms and applications," *Neural Netw.*, vol. 13, nos. 4–5, pp. 411–430, Jun. 2000.

[25] UCSD. (2021). *IClabel Tutorial: EEG Independent Component Labeling*. Accessed: Jan. 3, 2021. [Online]. Available: https://labeling.ucsd.edu/tutorial/labels

[26] A. Hekmatmanesh, H. Wu, A. Motie-Nasrabadi, M. Li, and H. Handroos, "Combination of discrete wavelet packet transform with detrended fluctuation analysis using customized mother wavelet with the aim of an imagery-motor control interface for an exoskeleton," *Multimedia Tools Appl.*, vol. 78, pp. 30503–30522, May 2019.

[27] A. Hekmatmanesh, H. Wu, M. Li, A. M. Nasrabadi, and H. Handroos, "Optimized mother wavelet in a combination of wavelet packet with detrended fluctuation analysis for controlling a remote vehicle with imagery movement: A brain computer interface study," in *New Trends in Medical and Service Robotics*. Springer, 2019, pp. 186–195.

[28] D. Q. Phung, D. Tran, W. Ma, P. Nguyen, and T. Pham, "Using Shannon entropy as EEG signal feature for fast person identification," in *Proc. ESANN*, 2014, vol. 4, no. 1, pp. 413–418.

[29] A. Hekmatmanesh, R. M. Asl, H. Wu, and H. Handroos, "EEG control of a bionic hand with imagination based on chaotic approximation of largest Lyapunov exponent: A single trial BCI application study," *IEEE Access*, vol. 7, pp. 105041–105053, 2019.

[30] N. Kannathal, M. L. Choo, U. R. Acharya, and P. Sadasivan, "Entropies for detection of epilepsy in EEG," *Comput. Methods Programs Biomed.*, vol. 80, no. 3, pp. 187–194, 2005.

[31] A. Hekmatmanesh, M. Mikaeili, K. Sadeghniiat-Haghighi, H. Wu, H. Handroos, R. Martinek, and H. Nazeran, "Sleep spindle detection and prediction using a mixture of time series and chaotic features," *Adv. Electr. Electron. Eng.*, vol. 15, no. 3, pp. 1–14, Oct. 2017.

[32] H. Niknazar, A. M. Nasrabadi, and M. B. Shamsollahi, "Volumetric behavior quantification to characterize trajectory in phase space," *Chaos, Solitons Fractals*, vol. 103, pp. 294–306, Oct. 2017.

[33] F. Takens, "Detecting strange attractors in turbulence," in *Dynamical Systems and Turbulence, Warwick 1980*. Springer, 1981, pp. 366–381.

[34] N. H. Packard, J. P. Crutchfield, J. D. Farmer, and R. S. Shaw, "Geometry from a time series," *Phys. Rev. Lett.*, vol. 45, no. 9, p. 712, Sep. 1980.

[35] A. Hekmatmanesh, R. M. Asl, H. Handroos, and H. Wu, "Optimizing largest Lyapunov exponent utilizing an intelligent water drop algorithm: A brain computer interface study," in *Proc. 5th Int. Conf. Event-Based Control, Commun., Signal Process. (EBCCSP)*, May 2019, pp. 1–5.

[36] R. Genuer, J.-M. Poggi, and C. Tuleau-Malot, "Variable selection using random forests," *Pattern Recognit. Lett.*, vol. 31, no. 14, pp. 2225–2236, Oct. 2010.

[37] W. Lin, Z. Wu, L. Lin, A. Wen, and J. Li, "An ensemble random forest algorithm for insurance big data analysis," *IEEE Access*, vol. 5, pp. 16568–16575, 2017.

[38] V. N. Vapnik, "Methods of pattern recognition," in *The Nature of Statistical Learning Theory*. Springer, 2000, pp. 123–180.

[39] V. Vapnik, *The Nature of Statistical Learning Theory*. Springer, 2013.

[40] A. B. Goldberg and X. Zhu, "New directions in semi-supervised learning," Ph.D. dissertation, Univ. Wisconsin-Madison, Madison, WI, USA, 2010.

[41] A. Hekmatmanesh, H. Wu, F. Jamaloo, M. Li, and H. Handroos, "A combination of CSP-based method with soft margin SVM classifier and generalized RBF kernel for imagery-based brain computer interface applications," *Multimedia Tools Appl.*, vol. 79, pp. 17521–17549, Feb. 2020.

[42] A. Hekmatmanesh, F. Jamaloo, H. Wu, H. Handroos, and A. Kilpeläinen, "Common spatial pattern combined with kernel linear discriminate and generalized radial basis function for motor imagery-based brain computer interface applications," in *Proc. AIP Conf.*, Apr. 2018, vol. 1956, no. 1, Art. no. 020003.

[43] X. Feng, J. Yang, F. Luo, J. Chen, and X. Zhong, "Automatic modulation recognition by support vector machines using wavelet kernel," in *Proc. J. Phys. Conf.*, Oct. 2006, vol. 48, no. 1, p. 1264.

[44] C. J. C. Burges, "A tutorial on support vector machines for pattern recognition," *Data Mining Knowl. Discovery*, vol. 2, no. 2, pp. 121–167, Jan. 1998.
[45] S. M. R. Noori, A. Hekmatmanesh, M. Mikaeili, and K. Sadeghniiat-Haghighi, "K-complex identification in sleep EEG using MELM-GRBF classifier," in *Proc. 21st Iranian Conf. Biomed. Eng. (ICBME)*, Nov. 2014, pp. 119–123.
[46] M.-P. Hosseini, A. Hosseini, and K. Ahi, "A review on machine learning for EEG signal processing in bioengineering," *IEEE Rev. Biomed. Eng.*, vol. 14, pp. 204–218, 2021.
[47] C. S. Pereira, J. Teixeira, P. Figueiredo, J. Xavier, S. L. Castro, and E. Brattico, "Music and emotions in the brain: Familiarity matters," *PLoS ONE*, vol. 6, no. 11, Nov. 2011, Art. no. e27241.
[48] R. A. Andersen and H. Cui, "Intention, action planning, and decision making in parietal-frontal circuits," *Neuron*, vol. 63, no. 5, pp. 568–583, Sep. 2009, doi: 10.1016/j.neuron.2009.08.028.
[49] Newsweek. (2021). *Pushing the Buy Button*. Accessed: Jan. 3, 2021. [Online]. Available: https://www.newsweek.com/pushing-buy-button-123737

ATEFE HASSANI received the B.Sc. degree in electrical engineering from the University of Zanjan, Iran, in 2017, and the M.Sc. degree in biomedical engineering from Shahed University, Tehran, Iran, in 2020. She is currently a Visiting Researcher with the Bio-Imaging Laboratory, University of Antwerp, Belgium. Her current research interests include biomedical signal processing, machine learning, deep learning, and computational neuroscience.

AMIN HEKMATMANESH received the bachelor's degree in electrical engineering from the Science and Research of Fars University, Shiraz, Iran, 2010, the master's degree in biomedical engineering from Shahed University, Tehran, Iran, in 2013, and the Ph.D. degree in brain-controlled ankle foot and hand orthosis and mobile vehicle robots using the EEG from the Laboratory of Intelligent Machines, Lappeenranta University of Technology, in 2019. His master's thesis was about analyzing sleep EEG signal processing, learning and negative emotional memory. Since 2020, he has been working as a Postdoctoral Researcher on heavy machine operator's health monitoring and signal processing for horse simulators at the Laboratory of Intelligent Machines, Lappeenranta University of Technology.

ALI MOTIE NASRABADI received the B.Sc. degree in electronic engineering and the M.Sc. and Ph.D. degrees in biomedical engineering from the Amirkabir University of Technology, Tehran, Iran, in 1994, 1999, and 2004, respectively. In 2004, he joined the Biomedical Engineering Department, Faculty of Engineering, Shahed University, where he was an Assistant Professor, from 2004 to 2011, an Associate Professor, from 2011 to 2017, and has been a Full Professor, since 2017. He is currently a Scientific Advisor with the National Brain Mapping Laboratory, University of Tehran, Tehran. His current research interests include brain–computer interfaces, biomedical signal processing, machine learning, deep learning, nonlinear time series analysis, and computational neuroscience. He is a Board Member of the Iranian Society for Biomedical Engineering and has served on the scientific committees for several national conferences and review boards of five scientific journals.